Proceedings Eighth Workshop Geothermal Reservoir Engineering
Stanford University, Stanford, California, December 1982
SGP-TR-60

# RESERVOIR CHARACTERIZATION OF THE RIBEIRA GRANDE (AZORES) FIELD

Mete, Luigi, Aquater, Spa, Italy

Rivera-Rodríguez, Jesús, Universidad Nacional Autónoma de México

## ABSTRACT

A description is made of the geothermal system located at the Ribeira Grande area in San Miguel Island at Azores. To date, three deep wells have been drilled, two of them are considered to be productive and the other one, although capable of production, has been used as an observation well due to completion problems.

One of the wells is presently connected to a 3 MW-portable power plant. A series of tests including both production and well testing, have been conducted in order to provide a reservoir characterization of the system. Several injection falloff, two rate and multiple rate tests have been carried out, as well as a preliminary interference--type test. A description of results obtained is provided.

## INTRODUCTION

Once a geothermal field has been located and confirmed by drilling several wells, it is convenient to establish several reservoir and fluid parameters which can be used in order to define the main characteristics of the geothermal system. These data are obtained from geological, geophysical, geochemical and reservoir engineering studies. All the information obtained from these studies should be considered in order to define a preliminary model of the system. Based upon this model and taking into account the main features and anisotropies of the system, as well as fluid characteristics, pressure and temperature, it is possible to come out with a reasonable preliminar assessment of the electrical potential of the geothermal field. This paper summarizes the results of the reservoir engineering studies and test performed on the existing wells of the Ribeira Grande Field in order to characterize the known portion of the system.

References and illustrations at end of paper.

## GENERAL BACKGROUND

The Ribeira Grande Field is located in the Sao Miguel Island at Azores (Fig. 1). Three deep wells have been drilled to date, the depth of these wells is 811, 887 and 1229 m, respectively. The geothermal system is located within igneous rocks. a Typical sequence found during drilling in the area under development includes alternate layers of lavas and pyroclastic products of trachytic composition in the shallowest zone, going through alternate layers of lavas and pyroclastites of intermediate composition, which then changes to alternate layers of lavas and pyroclastites of basaltic composition found at the production zone.

In the Ribeira Grande area there are many thermal manifestations, as well as in several places around the island. These features are related to tectonic activity and are located near faults and fractured zones. Two of the deep wells were located near one of such

manifestations. Figure 2 illustrates the location of wells and the main fault system in the area under exploitation.

Figure 3 shows the completion of well $PV_1$ as well as static pressure and temperature profiles and the main lithologic characteristics found while drilling this well. The Ribeira Grande reservoir is a liquid-dominated system whose production zone is located below 450 m in $PV_1$. The main production is thought to come through fractures.

At the beginning of the project and in spite of the fact that three deep wells had already been drilled, there was not a proper knowledge of what the reservoir was nor the thickness and the location of the producing intervals. There were only scarse and very preliminary data about the producing capacity of the wells available and the characteristics of their fluids, Therefore, it was the aim of the study undertaken to perform tests and data gathering to collect information realiable enough so as to come out with a proper characterization of the geothermal system. Geological, geophysical, geochemical, geohydrological and well testing studies were carried out. From all of them, this paper deals only with results obtained from the latter.

## WELL TESTING PROGRAM

The well testing program for this field was designed according to the following objectives: To locate depth and thickness of the producing zone(s) for each one of the wells available; to obtain the capacity (kh product) of the formation and to determine as occurate as possible both the productivity and the optimum orifice-size production diameter for each well, taking into account that they should be connected to a 3 MW-portable power plant, with a specified inlet steam pressure. An additional task defined during the progress of the field work was to establish even in a very rough manner, the connectivity of that part of the reservoir laying in between the wells available. Unfortunately, this aim could only be partially completed, as will be described later.

Additional restrictions to the type of well testing procedures available, that could be applied to this field were imposed by limitations in equipment availability at the well site, both in quantity and diversity. On the other hand, there were strong indications of a rapid scaling growth in the wells with hot brine production.

Among all pressure transient analysis techniques published in the literature[1], and keeping in mind, all restrictions mentioned above and the objectives pursued, it was decided to perform injection-falloff[2] and two-rate[3] and multiple-rate production testing. This program was carried out in conjunction with well-productivity tests.

## INJECTION-FALLOFF TESTS

Injection tests were carried out for two reasons, first to determine the location and thickness of permeable zones within the wellbore open interval, and second for measuring formation capacity (kh). Fig. 4 shows temperature distribution in well $PV_1$, before injection and also the distribution found from a temperature survey conducted 6 hours after water injection ended. Analyzing this figure permeable zones become apparent.

Injection tests were performed following well-established techniques[1,2]. Just for the sake of completeness, a brief description follows. The standard procedure was to inject fresh water to a prefixed rate for a period of three to four hours, recording changes in bottom-hole pressure by means of a standard bourdon-tube type pressure bomb. Immediately after injection stops, bottom-hole, pressure was recorded during the fallof period for at least twice the injection time. Therefore, it was possible to perform the analysis using

both injection and falloff data in order to check results obtained. Interpretation techniques are well-known and the reader is refered elsewhere[1,2] for futher detail. Fig. 5 shows data for an injection-falloff test performed in well $PV_1$.

Once the duration of wellbore storage effects[1,4] were determined by means of type-curve procedures, semi-log analysis techniques were carried out. As far as type-curve procedures is concerned, those presented by Agarwal et al[5] and Gringarten et al[6] were performed. These techniques were used only as cheking devices for results obtained by means of analytical methods or when conditions for an adequate application of these methods were not reached.

Dimensionless pressure and time are defined according to Agarwal et al[5] as follows*:

$$p_D = \frac{kh}{141.2q\mu B}\,\Delta p \quad \ldots \quad (1)$$

$$t_D = \frac{0.0002637\,k}{\phi\mu c_t r_w^2}\,t \quad \ldots \quad (2)$$

in a similar manner, the dimensionless wellbore storage parameter is given by:

$$c_D = \frac{0.8936\,C}{\phi c_t h r_w} \quad \ldots \quad (3)$$

where C is the wellbore storage constant.

Figure 5 and 6 show the match obtained by fitting field data obtained during the falloff period of an injection test performed on well $PV_1$. Fig. 5 correspond to a match on type-curves published by Agarwal et al[5] and Fig. 6 illustrates the match obtained by using type-curves presented by Gringarten et al[6]. Data for this test is shown in Table 1.

* Nomenclature at end of paper.

It was observed from the injection-fall off tests performed in this field that matching field data to the type curves of Gringarten et al was easier than when the match was made by means of Agarwal et al curves. Field data points measured during the infinite acting period of the test were well developed and relatively easy to adjust to one of the curves of Gringarten et al correlation, when plotted as $\Delta p$ vs. $\Delta t$, as shown in Fig. 7. On the other hand, when Agarwal et al type-curve was used, it was observed that the match was not unique. In fact, field data points could have been fitted to curves having different values of $C_D$ and s. This is because different curves on this correlation have similar shapes. However, once the wellbore storage constant was evaluated, a good and unique match was obtained, as shown in Fig. 6. The permeability-thickness product (kh) product was calculated from the pressure match, as illustrated in Appendix. Good agreement was obtained from both matches and results also agreed with those obtained from semi-log techniques. Table 2 summarizes these results for well $PV_1$.

Although fluid production from this field is most probably obtained from a combination of flow through fractures, fissures and interbedding planes of several lava flows, the high value of the skin factor obtained (s on the order of 20), was explained on the basis of several known factors.

Firstly, the injection-falloff test was carried out in well $PV_1$ shortly after a clean-up workover in this well was performed, and before any fluid production took place. This workover had to be undertaken because severe scaling in the well was detected, which had closed almost completely the wellbore after several short duration production periods[7]. Therefore, it seemed a reasonable assumption to consider that at least part of the scaling products removed from the wellbore during workover could have gone into the fracture

zones. In addition to this, surface chemical sampling provided a preliminary indication towards the possibility of some scaling deposition in the vicinity of the wellbore. A detailed geochemical sampling and additional well testing, was submited in order to properly define scaling mechanism and to indicate possible solutions to the problem[7].

After the start of the semi-log straight line has been determined, conventional well test interpretation techniques were used. This kind of analysis is well known and the basic equations are as follows[1,2]:

For a constant rate injection test, bottom-hole pressure is given as:

$$p_{wf} = p_{1hr} + m \log t \quad \ldots \quad (4)$$

The skin factor, s, is a follows:

$$s=1.1513\left[\frac{p_{1hr}-p_i}{m} - \log\left(\frac{k}{\phi\mu c_t r_w}\right)+ 3.2275\right]. \quad (5)$$

where:

$$p_{1hr}=p_i + m\left[\log\left(\frac{k}{\phi\mu c_t r_w^2}\right)-3.2275+0.86859s\right] \quad (6)$$

$$m = - \frac{162.6\ qB\mu}{kh} \quad \ldots \quad (7)$$

In a similar manner, bottom-hole pressure during falloff following a constant injection period is given by the following equation:

$$p_{ws} = p^* - m \log\left(\frac{t_p + \Delta t}{\Delta t}\right) \quad \ldots \quad (8)$$

From this equation it is evident that a plot of $p_{ws}$ vs $\log\left(\frac{t_p + \Delta t}{\Delta t}\right)$, should produce a straight line whose slope is given by the following equation:

$$m = \frac{162.6\ qB\mu}{kh} \quad \ldots \quad (9)$$

The skin factor is as follows:

$$s=1.1513\left[\frac{p_{1hr}-p_{wf}(\ t=0)}{m} - \log\left(\frac{k}{\phi\mu c_t r_w^2}\right)+3.2275\right]$$

$$\ldots \quad (10)$$

Fig. 8 shows a semi-log plot of $p_{ws}$ vs $\log\left(\frac{t + \Delta t}{\Delta t}\right)$.

The proper selection of the correct straight line is very important and is not always evident. Fig. 8 illustrates this point, where departure from the correct straight line is belived to be due mainly to thermal effects, without discarding the presence of some kind of outer boundary. The Appendix shows calculations by the semilog method and Table 2 summarizes results.

## TWO-RATE AND MULTIPLE-RATE TESTING

To check kh values obtained from injection-falloff tests, two-rate and multiple-rate production tests were scheduled for wells in the Ribeira Grande Field. For a detailed description of the methodology involved, the reader is refered elsewhere[1,3].

Fig. 9 shows data from a two-rate flow test performed in well $PV_1$. This test was carried out following procedures previously described in reference 3. Before this test was conducted, the flashing point within the wellbore was properly located and the pressure bomb was set approximately 100 m below this point, so as to ensure the presence of only one-phase below the recording point during the duration of the test. Results were interpreted by using Russell[8], Selim[9] and Odeh and Jones[10] models, whose equations are listed below[3]:

a) Russell Model

$$p_{wf} = p_i - 527.4\frac{w_2 \nu_{sc} B\mu}{kh}\left(\log\frac{k}{\phi\mu c_t r_w^2}\right.$$

$$+ 0.891 + 0.87\ s)$$

$$- 527.4 \frac{w_1 \nu_{sc} B}{kh} \left(\log \frac{t+\Delta t'}{\Delta t'} + \frac{w_2}{w_1} \log \Delta t'\right) \quad \ldots (11)$$

From eq. (11) it is evident that by plotting $p_{wf}$ vs $\left(\log \frac{t + \Delta t'}{\Delta t'}\right) + \frac{w_2}{w_1} \log \Delta t'$ a straight line is obtained. The slope of this line is given by:

$$m_R = 527.4 \frac{w_1 \nu_{sc} B\mu}{kh} \quad \ldots (12)$$

Figure 10 shows a graph prepared according to Russel's model.

b). Selim Model

Selim[9] suggested modification of the method proposed by Russell[8], by returning the well to the producing rate it had prior to the test once the well had reached stable conditions. The pressures and flow rates should be measured until new stabilized conditions are reached. The equation for this model is as follows:

$$p_{wf} = p_i - 527.4 \frac{w_1 \nu_{sc} B\mu}{kh} \left(\log \frac{k}{\phi \mu c_t r_w^2} + 0.891 + 0.87\ s\right) - 527.4 \frac{w_2\ sc B}{kh} \left(\log \frac{\left(\frac{w_1}{w_2}\right) t+\Delta t'+\Delta t''}{\Delta t''} + \frac{w_3}{w_2} \log \Delta t''\right) \quad \ldots (13)$$

From Eq. 13 it is evident that plotting $p_{wf}$ vs. $\left(\log \left[\frac{\left(\frac{w_1}{w_2}\right) t+\Delta t'+\Delta t''}{\Delta t''}\right] + \frac{w_3}{w_2} \log \Delta t''\right)$ a straight line is obtained whose slope is

$$m_S = \frac{527.4 \nu w_2\ sc B\mu}{kh} \quad \ldots (14)$$

Figure 11 illustrates the graph obtained according to this model. There is an additional constraint that $m_R$ and $m_S$ should satisfy. This constraint is as follows:

$$\frac{m_R}{m_S} = \frac{w_1}{w_2} \quad \ldots (15)$$

Eq. (15) can be used to select the appropiate straight line portion in the event that several straight lines are present due to scatter of field data.

c) Odeh and Jones Variable Drawdown Model

The field data obtained during the transient conditions after the change in rate were analyzed as a variable drawdown case having $w_1$ and $w_2$ as the initial and final flow rates. The interpretation equation is as follows:

$$\frac{p_i - p_{wf}}{w_n} = 527.4 \frac{\nu_{sc} B\mu}{kh} \sum_{i=0}^{n-1} \frac{\Delta w_i}{w_n} \log(t_n - t_i) + 0.8926 + 0.87s + \log \frac{k}{\phi \mu c_t r_w^2} \quad \ldots (16)$$

Therefore, by graphing

$$(p_i - p_{wf}) \text{ vs } \sum_{i=0}^{n-1} \frac{\Delta w_i}{w_n} \log (t_n - t_i),$$

a straight line is obtained whose slope is given by the following equation:

$$m_{OJV} = 527.4 \frac{\nu_{sc} B\mu}{kh} \quad \ldots (17)$$

Fig. 12 shows the graph obtained when field data are plotted according to this model. Table 3 summarizes results obtained by applying the models mentioned above.

Equations (11) through (17) are expressed in metric geothermal units and flow rates are in terms of mass, rather than volume. For these equations the meaning of flow rates is as follows:

$w_1$ = Stabilized mass flow rate prior first rate change, ton/hr

$w_2$ = Stabilized mass flow rate after first rate change, ton/hr

$w_3$ = Stabilized mass flow rate after second rate change, ton/hr

All other variables are listed on the Nomenclature section.

## INTERFERENCE TYPE TEST

It was considered of great importance to conduct a very rough interference test between wells $PV_1$, and $PV_2$ (see Fig. 2 for well locations). This attempt was carried out in spite of not disposing of adequate instrumentation such as high-precision bottom-hole pressure sensing and recording devices, such as the ones used in similar field applications[11].

It was decided to detect bottom-hole pressure changes in well $PV_2$, induced by fluid extraction from its neighbor well $PV_1$. Changes in pressure were detected, by means of the more precise Bourdon-type bottom-hole pressure recording device available, keeping in mind the range of resolution of this instrument. This attempt was encouraged also from evidences of interference of well $PV_2$ production on the productivity of well $PV_1$, when both were simultaneously under exploitation[12].

Fig. 13 shows the few meaningful data points obtained from this test after data filtration. An attempt to match this data with the exponential integral solution[13] is illustrated in Fig. 13. As it is evident, by using the few data available, three different matches could be made. Table 4 summarizes results obtained.

## CONCLUSIONS

Based upon the results obtained from the well testing program carried out at the Ribeira Grande Geothermal Field and briefly described in this paper, the following conclusions can be drawn:

1. Reservoir characterization is a very important step in the adequate knowledge of the anisotropies and main features of a given geothermal field. This knowledge will definetely contribute towards a more precise definition of the electrical generation capacity of a reservoir.

2. Injection-falloff tests provide a useful tool for locating permeable zones in either igneous or sedimentary rocks and also to evaluate their capacity.

3. Two-rate flow testing can be applied to obtain basic reservoir parameters.

## NOMENCLATURE

B = brine formation volume factor, (volume, reservoir conditions/volume, standard conditions).

C = wellbore storage constant, bbl/psi

$C_D$ = dimensionless wellbore storage coefficient.

$c_t$ = total compressibility, $(psi)^{-1}$

h = formation net thickness, ft.

k = permeability, md.

m = slope of a straight line

p = pressure, psi.

$p_i$ = initial pressure, psi.

$p_{wf}$ = flowing bottom-hole pressure, psi.

$p_{1hr}$ = flowing bottom-hole pressure al 1hr,psi

$p_{ws}$ = static bottom-hole pressure, psi.

$p_D$ = dimensionless pressure.

$p^*$ = false pressure, pressure obtained when linear portion of the plot of $p_{ws}$ vs. $\log[(tp+\Delta t)/\Delta t]$ is extrapolated to $(tp+\Delta t)/\Delta t=1$, psi.

GREEK SYMBOLS

$\mu$ = viscosity, cp.
$\nu$ = specific volume, $cm^3/gr$
$\phi$ = porosity, fraction

For the two-rate flow test (equations (11) through (17), geothermal metric units were used. Therefore, for these equations, the following nomenclature was used.

B = brine formation volume factor, (volume, reservoir conditions / volume, standard conditions)
c = total fluid compressibility, $(kg/cm^2)^{-1}$
h = formation net thickness, m
k = permeability, md
m = slope of a straight line
n = constant rate intervals in Odeh and Jones model
p = pressure, $kg/cm^2$
$p_i$ = initial pressure, $kg/cm^2$
$p_{wf}$ = flowing bottom-hole pressure, $kg/cm^2$
$p_{1hr}$ = flowing bottom-hole pressure 1 hr after the rate change, $kg/cm^2$
q = volumetric flow rate, bbl/day
$r_w$ = wellbore radius, cm
s = skin factor, dimensionless
t = producing time to instant of rate change, hrs
t' = producing time measured from first rate change, hrs
t" = producing time measured from second rate change, hr
w = mass flow rate, ton/hr
y = correlation parameter in Odeh and Jones method

SUBSCRIPTS

1 = conditions prior to rate change
2 = conditions after first rate change
3 = conditions after second change
i = initial condition
OJV= refers to Odeh and Jones variable draw down model
R = refers to Russell's model
S = refers to Selim's model
sc = standard conditions
w = wellbore
wf = flowing conditions

ACKNOWLEDGEMENTS

The authors wish to thank Mr. Antonio M. Rodríguez-da Silva, Director do Programa Geotérmico dos Açores, Lab. Geo. e Tecnologia, for permission to publish the field data presented in this paper. The encouragment and support from the management of Aquater is also acknowledged. We also appreciate the assistance from Mr. A. Drei in processing field data.

REFERENCES

1. Earlougher, R.C., Jr.: Advances in Well Test Analysis, Society of Petroleum Engineers of AIME Monograph Volume 5, Dallas, Tex. (1977).
2. Rivera-R., J. and Saltuklaroglu, M.:"Well Testing at Los Azufres Geothermal Field", paper SPE 8348 presented at the 54th Annual Fall Technical Conference and Exhibition of the Society of Petroleum Engineers of AIME, Las Vegas, Nevada (Sep.23-26, 1979).
3. Rivera-R., J., and Ramey, H.J., Jr.: "Application of Two-Rate Flow Tests to the Determination of Geothermal Reservoir Parameters", Paper SPE 6887 presented at SPE-AIME 52nd Annual Technical Conference, Denver, Colorado (Oct.9-12, 1977).

4. Miller, C.W.: "Wellbore Storage Effects in Geothermal Wells", Soc. Pet. Eng. Jour., (Dec. 1980) 555-566.

5. Agarwal, R.G., Al-Hussainy, R., and Ramey, H.J., Jr.: "An Investigation of Wellbore Storage and Skin Effect in Unsteady-Liquid Flow, I Analytical Treatment", Soc. Pet. Eng. Jour. (Sept. 1970) 279-290.

6. Gringarten, A.C., Bourdet, D.P., P.A. and Kniazeff, V.J.: "A Comparison Between Different Skin and Wellbore Storage Type-Curves for Early-Time Transient Analysis", Paper SPE 8205 presented at 54th Annual Fall Technical Conference and Exhibition of the Society of Petroleum Engineers of AIME, Las Vegas, Nevada (Sep. 23-26,1979)

7. Aquater, S.p.A.: Feasibility Study of Geothermal Power Plant of Ribeira Grande-S. Miguel, FIRST-STEP REPORT,Annex D-Well Testing, San Lorenzo In Campo, Italy, June 1982.

8. Russell, D.G.: "Determination of Formation Characteristics by Two-Rate Flow Tests", J. Pet. Tech., December 1962, 1347-1355.

9. Selim, M.A.: "A Modification of the Two-Rate Flow Method for Determination of Reservoir Parameters", J. Institute of Petroleum, v. 53, No. 527, (Nov. 1967) 343-352.

10. Odeh, A.S., and Jones, L.G.:"Pressure Drawdown Analysis, Variable Rate Case", J. Pet. Tech., (Aug. 1965) 960-964.

11. Rivera-R., J., Samaniego-V., F. and Schroader, R.C.: "Pressure Transient Testing at Cerro Prieto Geothermal Field", Geothermics, Vol. 9 (1980) 189-196.

12. Rodrigues-da Silva, A., private communication.

13. Earlougher, R.C., Jr., and Ramey, H.J., Jr.: "Interference Analysis in Bounded Systems", Jour. Can. Pet. Tech. (Oct.-Dec. 1973) 33-45.

## APPENDIX

### A. Falloff test calculations

1. Type-curve procedures.

a) Agarwal et al

From the pressure match shown on Fig. 6, and from eq. (1), once the adequate transformation of units has been made, it follows:

Match point:

For $(t)_M = 10$ min., $t_D = 8.6 \times 10^5$

For $(\Delta p)_M = 10$ Kg/cm$^2$ (142 psi), $p_D = 20.5$, $s = 20$

From eq. (1) in the text:

$$kh = 141.2\, qB\mu_w \frac{(p_D)_M}{(\Delta p)_M} = 141.2(4604)(1.06)$$

$$(0.28)\frac{(20.5)}{142} = 8500 \text{ md-m}$$

b) Gringarten et al

From the pressure match shown on Fig. 7, and from eq. (1), the following results are obtained:

Match point:

For $(t)_M = 10$ min, $\frac{t_D}{C_D} = 10.5$

For $(p)_M = 10$ Kg/cm$^2$ (142 psi), $p_D = 26.5$,

$$C_D e^{2s} = 10^{30}$$

From eq. (1) in the text:

$$kh = 141.2\, qB\mu_w \frac{(p_D)_M}{(\Delta p)_M} = 141.2\ (4604)(1.06)$$

$$(0.28)\ (\frac{26.5}{142}) = 10987 \text{ md-m}$$

2. Semi-log methods.

From Fig. 8, the slope of the semi-log straight line during falloff is:

$$m = 0.50 \frac{Kg/cm^2}{cycle} \left(7.1 \frac{psi}{cycle}\right)$$

Then, from eq. (1) in the text:

$$kh = \frac{162.6\ qB\mu_w}{m} = \frac{162.5(4604)(1.06)(0.22)}{(7.1)\ (3.28)}$$

$$= 7496 \text{ md-m } (24588 \text{ md-ft})$$

B. Two-Rate flow test calculations

a) Russell's Model

From Fig. 10, $m_R = 1.66$.

Then:

$$(kh)_R = \frac{527.4\ W_1\ \nu_{sc} B\mu_w}{m_R}$$

$$= \frac{(527.4)(108.53)(1.043)(1.18)(0.145)}{1.66}$$

$$(kh)_R = 7002 \text{ mdm}$$

b) Selim's Model

From Fig. 11, $m_s = 0.68$.

Then:

$$(kh)_s = \frac{527.4\ w_2\ \nu_{sc} B\mu_w}{m_s}$$

$$= \frac{(527.4)(59.14)(1.043)(1.18)(0.165)}{0.68}$$

$$(kh)_S = 9315 \text{ mdm}$$

From Fig. 12, $m_{OJV} = 0.0115$

Then:

$$(kh)_{OJV} = \frac{527.4\ \nu_{sc} B\mu_w}{m_{OJV}}$$

$$= \frac{527.4)(1.043)(1.18)(0.165)}{0.0115}$$

$$(kh)_{OJV} = 9313 \text{ mdm}$$

Table 1. Data for falloff test in well $PV_1$. $q_{inj}$=4604 bbl/day.

| Δt TIME (minutes) | BOTTOM-HOLE PRESSURE $p_{ws}$ (Kg/cm²) |
|---|---|
| 0 | 39.53 |
| 0.5 | 37.95 |
| 1 | 36.25 |
| 2 | 33.45 |
| 3 | 31.35 |
| 4 | 30.01 |
| 5 | 28.72 |
| 6 | 27.85 |
| 7 | 27.31 |
| 8 | 26.85 |
| 9 | 26.51 |
| 10 | 27.27 |
| 15 | 25.64 |
| 20 | 25.52 |
| 30 | 25.52 |
| 40 | 25.61 |
| 50 | 25.65 |
| 60 | 25.70 |
| 70 | 25.75 |
| 80 | 25.76 |
| 90 | 25.77 |
| 98 | 25.77 |
| CLOCK FAILURE | |
| 206 | 25.80 |
| 226 | 25.72 |
| 246 | 25.59 |
| 266 | 25.44 |
| 286 | 25.25 |
| 306 | 25.09 |
| 326 | 24.92 |
| 346 | 24.76 |

Table 2.- Results obtained from falloff test performed in well $PV_1$

| Interpretation Technique | Results | |
|---|---|---|
| | kh (md-m) | s |
| Type-curve matching (Agarwal et al.) | 8500 | 20 |
| Type-curve matching (Gringarten et al.) | 10987 | |
| Semi-log | 7496 | |

Table 3.- Results obtained from two-rate flow test carried out in well $PV_1$

| Interpretation Technique | kh (md-m) |
|---|---|
| Russell | 7002 |
| Selim | 9315 |
| Odeh & Jones | 9313 |

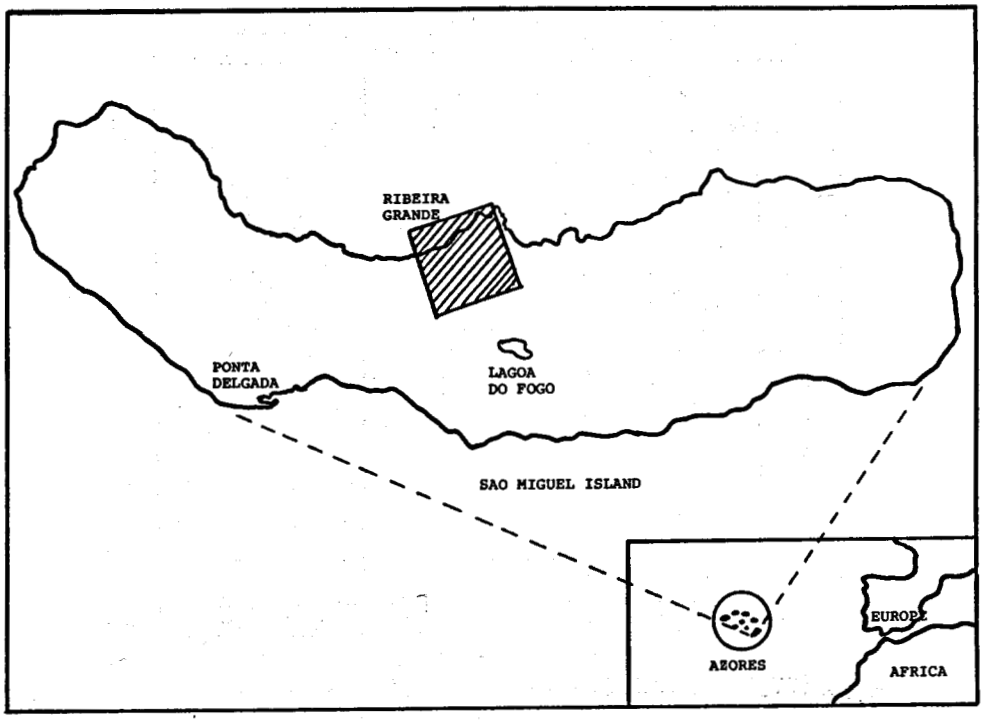


FIG. 1.-Location of the Ribeira Grande Geothermal Field

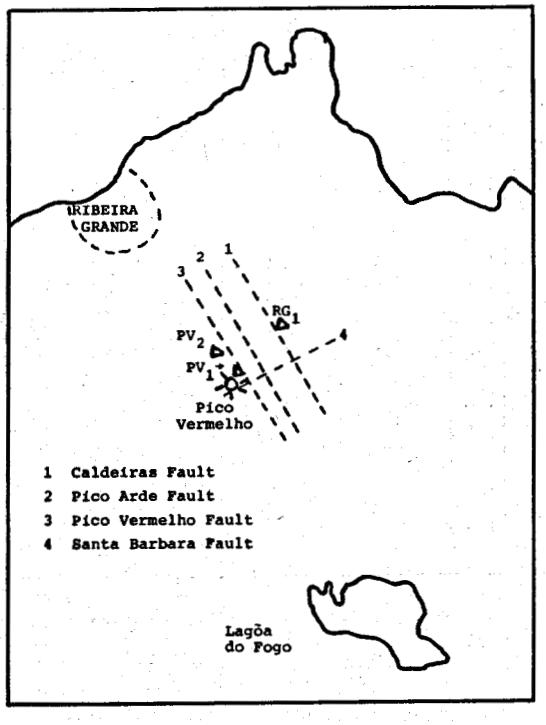


FIG. 2.-Main fault system associated with the Ribeira Grande Field

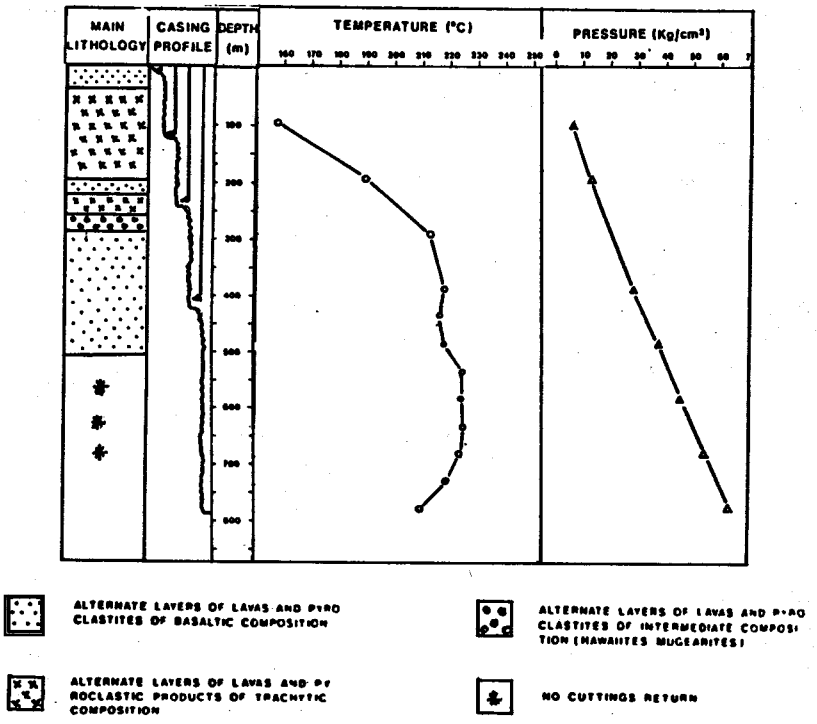


FIG. 3.-Well completion, lithology and pressure and temperature profiles for well $PV_1$

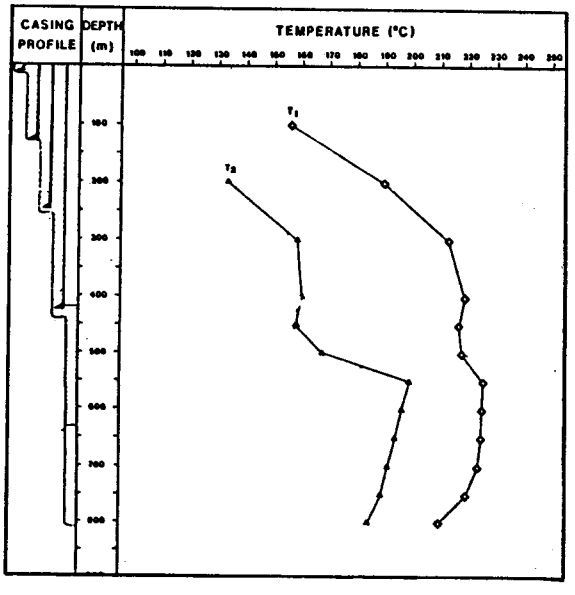


$T_1$ Static temperature profile

$T_2$ Temperature profile 6 hours after water injection stopped

FIG. 4.-Temperature profile before and after water injection in well $PV_1$

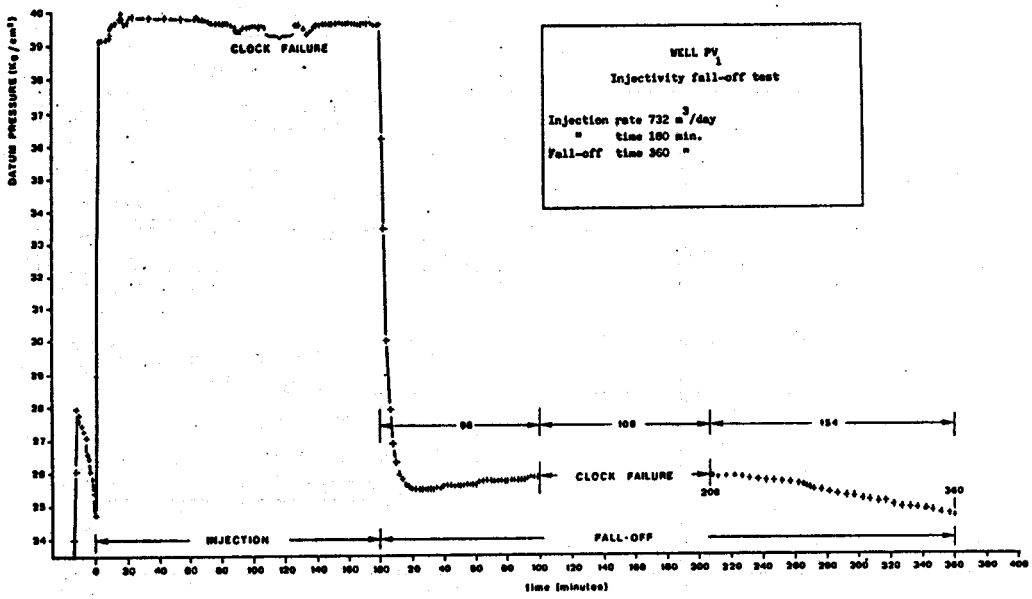


FIG. 5.-Datum pressure vs time - injectivity fall-off test

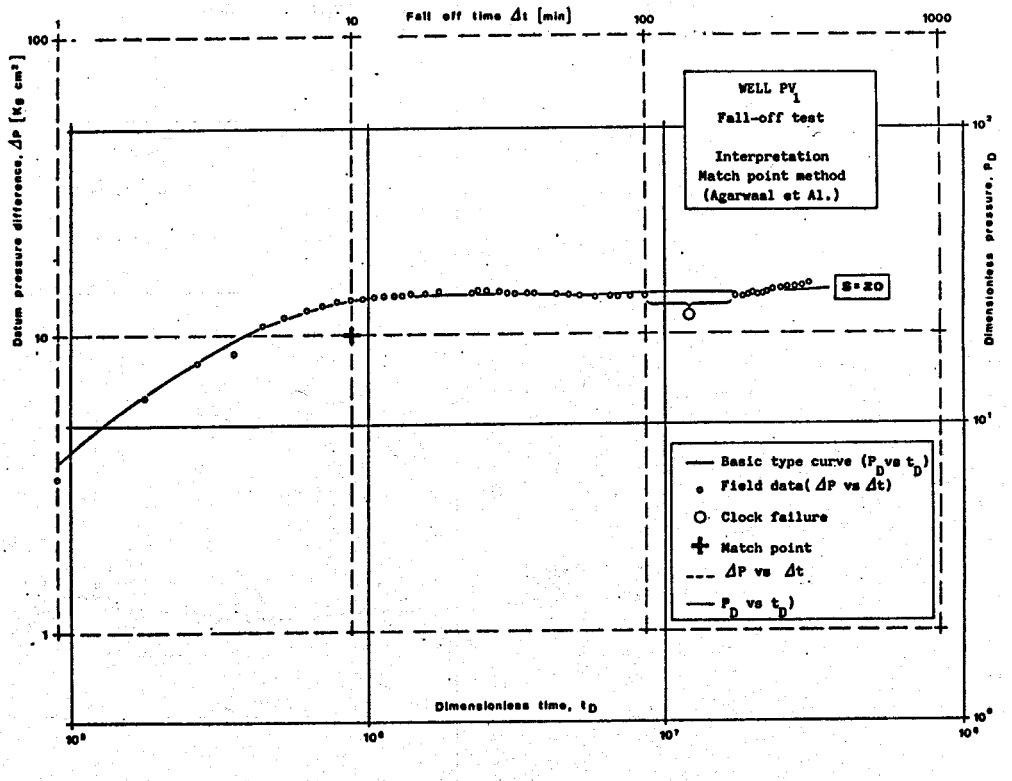


FIG. 6.-Datum pressure difference vs fall-off time; dimensionless pressure vs dimensionless time. log-log plots - fall-off test.

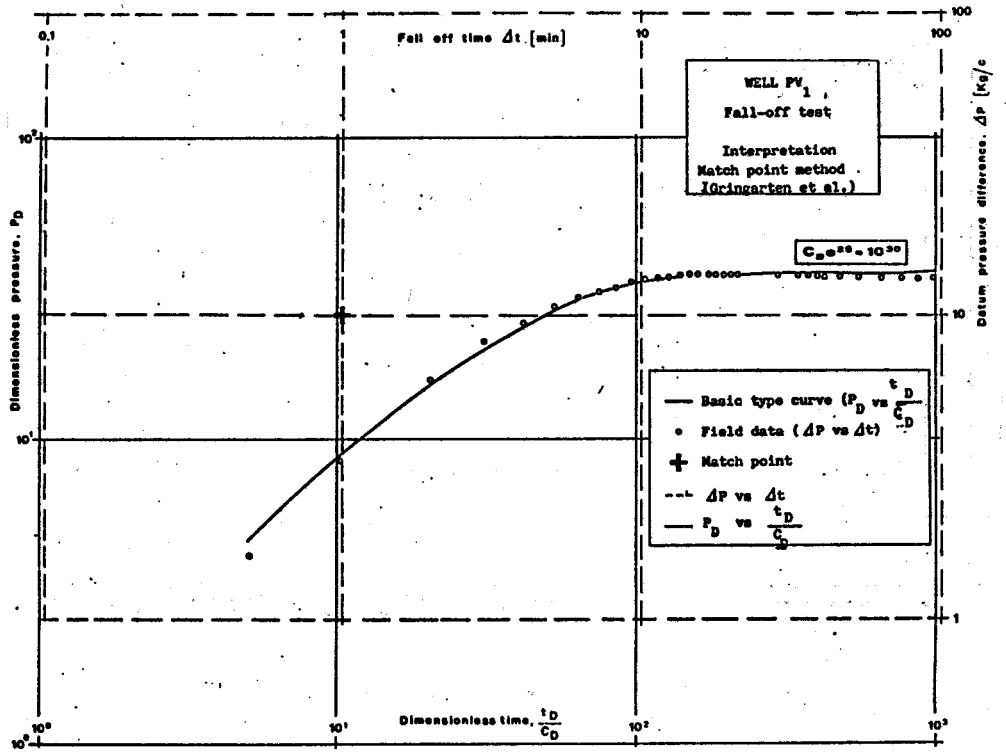


FIG. 7.-Datum pressure difference vs fall-off time; dimensionless pressure vs dimensionless time. log-log plots - fall-off test.

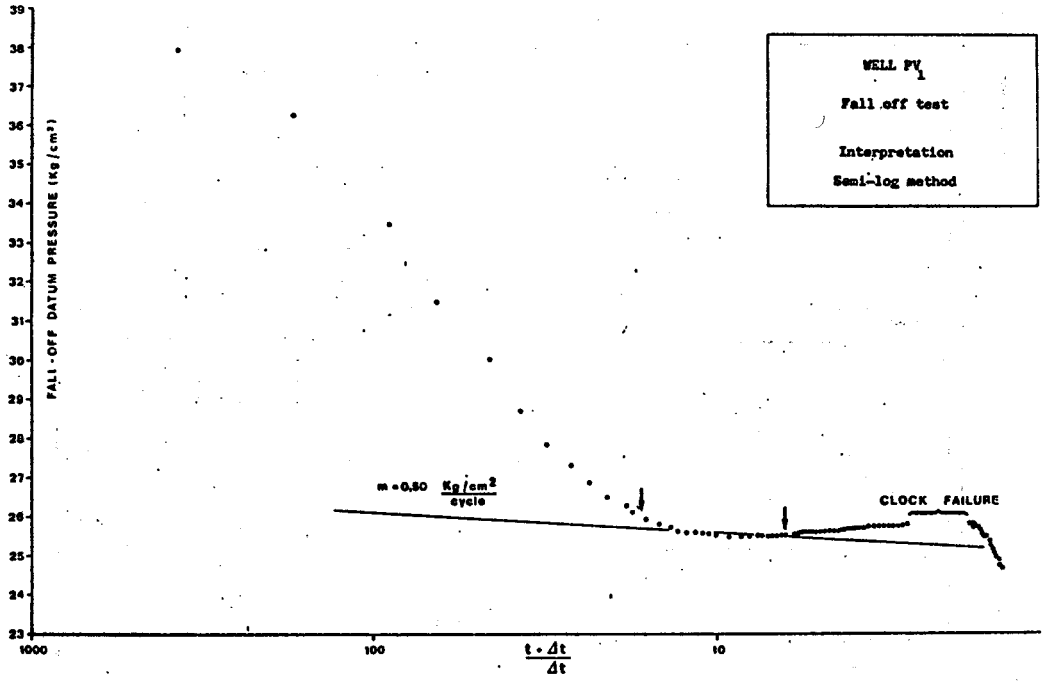


FIG. 8.-Datum pressure vs dimensionless time. Semi-log plot - fall-off test.

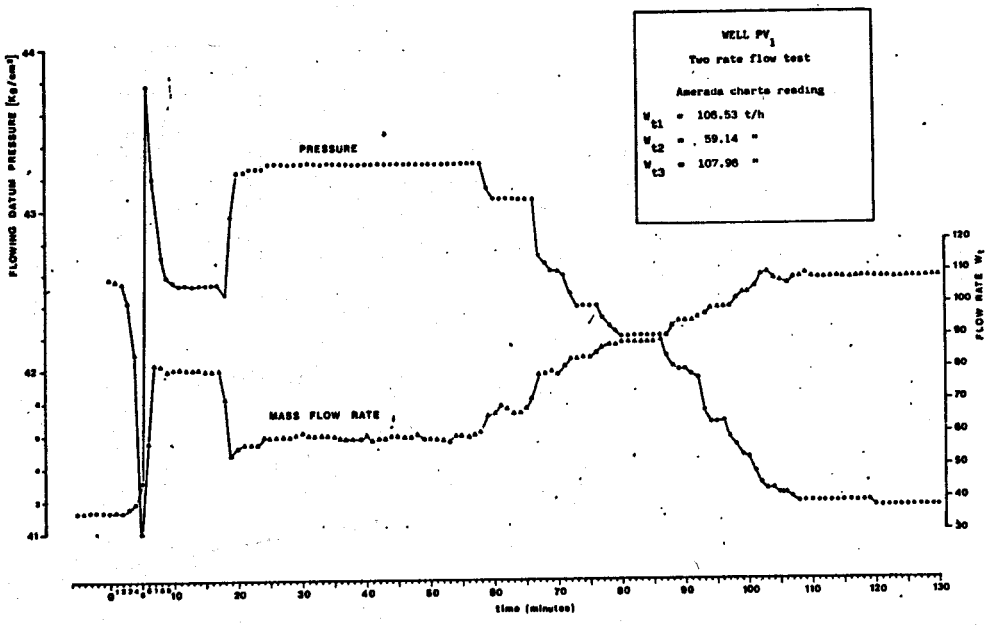


FIG. 9.-Flowing datum pressure vs time - two rate flow test

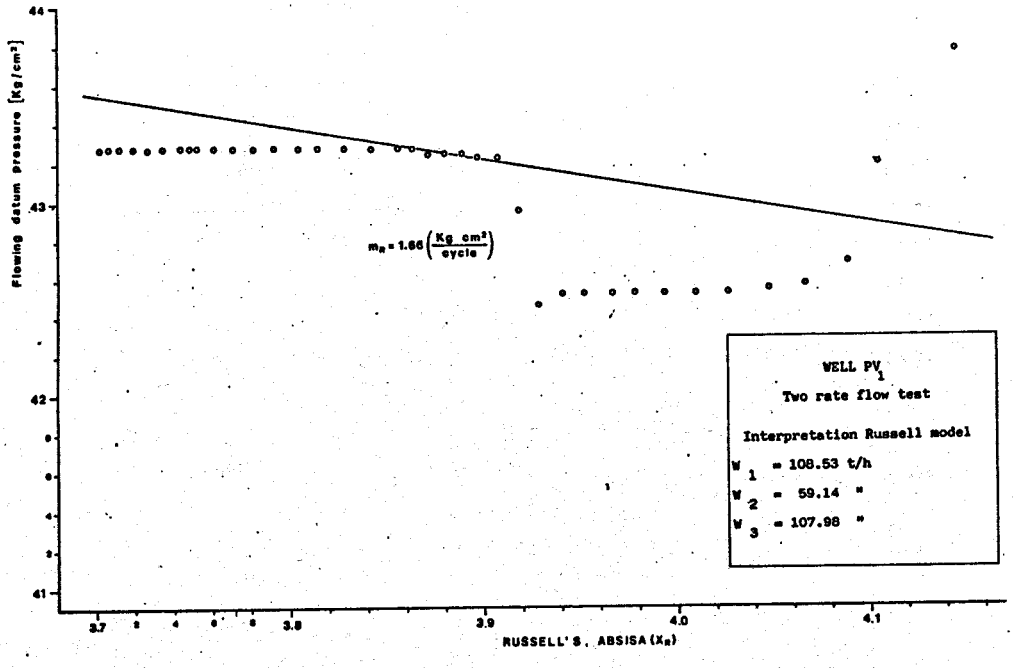


FIG. 10.-Flowing datum pressure $P_{wf}$, vs Russell's absisa ($X_R$) - two rate flow test

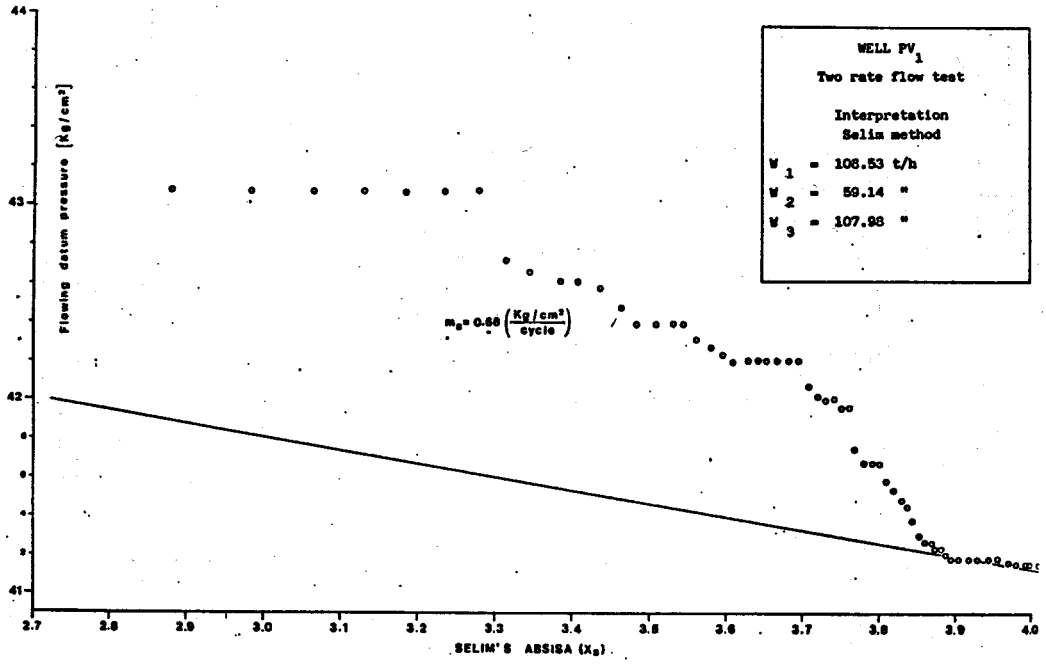


FIG. 11.-Flowing datum pressure $P_{wf}$ vs time - Selim's absisa $X_s$ - two rate flow test

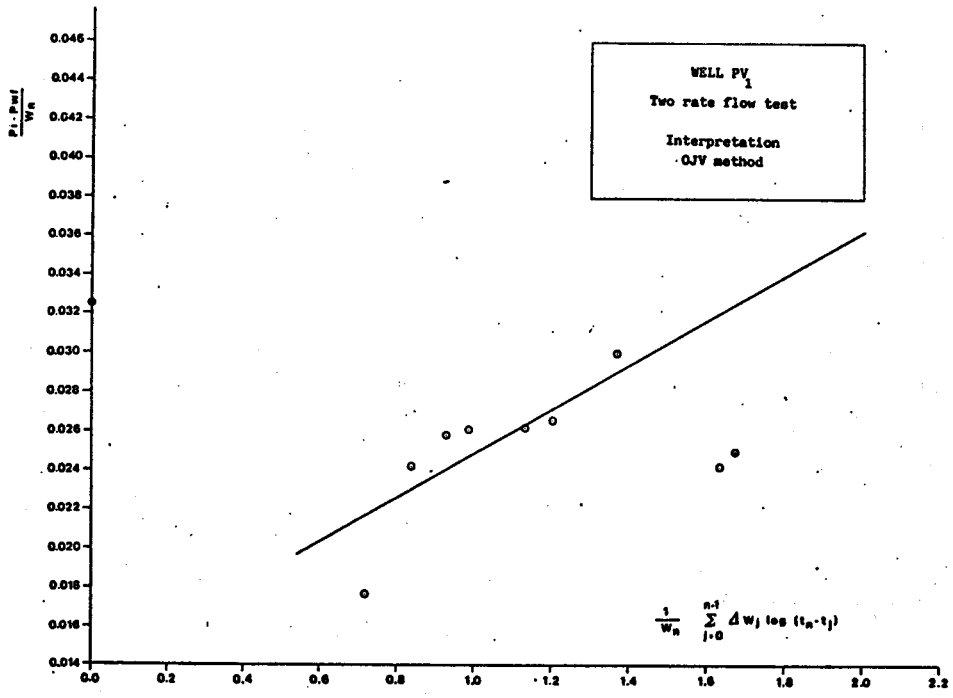


FIG. 12.-O.J.V. plot, two rate flow test.

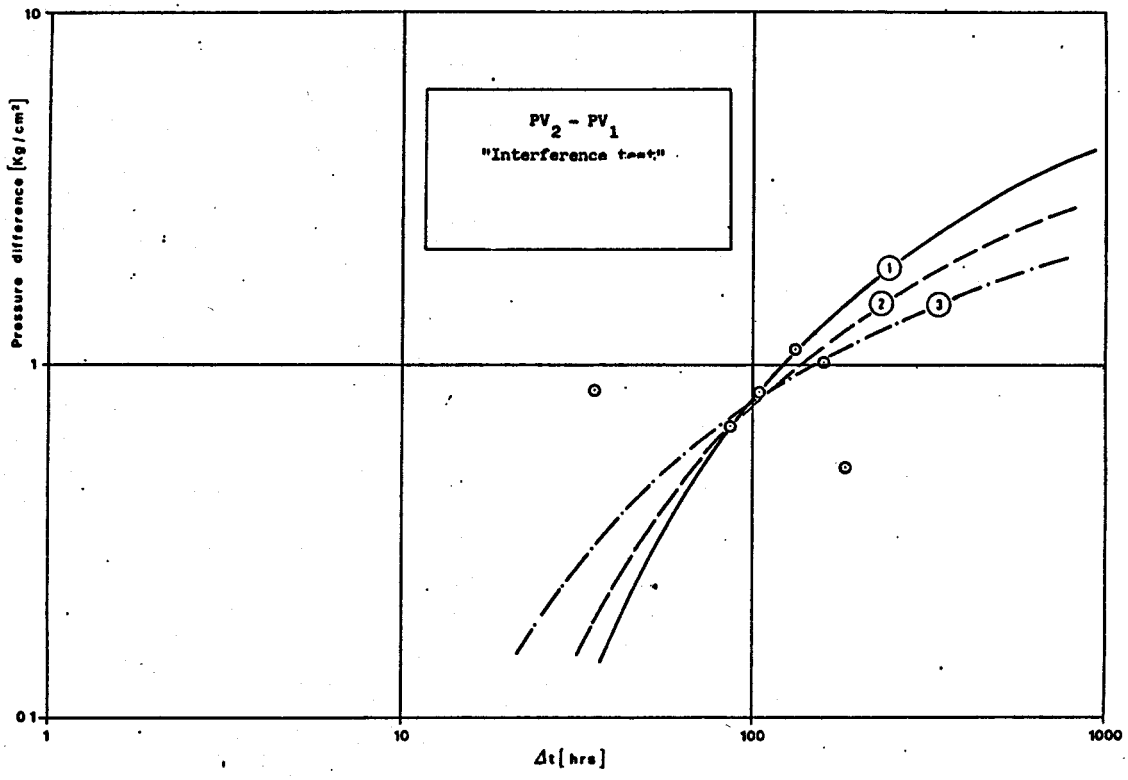


FIG. 13.-Pressure difference $\Delta P$ vs time - $PV_1$-$PV_2$ "Interference test".